9. Higashijima, T.; Burnier, J.; Ross, E. M. *J. Biol. Chem.* **1990**, *265*, 14176.
10. Oppi, C.; Wagner, T.; Crisari, A.; Camerini, B.; Valentini, G. P. T. *Proc. Natl. Acac. Sci. USA.* **1992**, *89*, 8268.
11. Ho, C. L.; Hwang, L. L. *Biochem. J.* **1991**, *274*, 453.
12. Ho, C. L.; Hwang, L. L.; Lin, Y. L.; Chen, C. T.; Yu, H. M.; Wang, K. T. *Eur. J. Pharmacol.* **1994**, *259*, 259.
13. Yu, H. M.; Wu, T. M.; Chen, S. T.; Ho, L. C.; Her, G. R.; Wang, K. T. *Biochem. Mol. Biol. Int.* **1993**, *29*, 241.
14. Park, N. G.; Yamato, Y.; Lee, S.; Sugihara, G. *Biopolymers.* **1995**, *36*, 793.
15. Chuang, C. C.; Huang, W. C.; Yu, H. M.; Wang, K. T. Wu, S. H. *Biochem. Biophys. Acta.* **1996**, *1292*, 1.
16. Higashijima, T.; Wakamatsu, K.; Saito, K.; Fujino, M.; Nakajima, T.; Miyazawa, T. *Biochem. Biophys. Acta* **1984**, *802*, 157.
17. Ben-Efraim, I.; Bach, D.; Shai, Y. *Biochemistry* **1993**, *32*, 2371.
18. Suenaga, M.; Lee, S.; Park, N. G.; Aoyagi, H.; Kato, T.; Umeda, A.; Amako, K. *Biochem. Biophys. Acta* **1988**, *981*, 143.
19. Weinstein, J. N.; Yoshikami, S.; Henkart, P.; Blementhal, R.; Hagins, W. A. *Science* **1977**, *195*, 489.
20. Wakamatsu, K.; Okada, A.; Miyazawa, T.; Ohya, M.; Higashijima, T. *Biochemistry* **1992**, *31*, 5654.
21. Eisenberg, D.; Weiss, R. W.; Terwilligar, T. C. *Nature* **1982**, *299*, 371.
22. Eisenberg, D. *Annu. Rev. Biochem.* **1984**, *53*, 595.
23. Kaiser, E. T.; Kézdy, F. J. *Annu. Rev. Biophys. Biophys. Chem. 1987*, *16*, 561.
24. Dowson, C. R.; Drake, A. F.; Helliwell, J.; Hider, R. C. *Biochim. Biophys. Acta* **1978**, *510*, 75.
25. Steiner, H.; Andreu, D.; Merrifield, R. B. *Biochim. Biophys. Acta* **1988**, *939*, 260.
26. Zasloff, M. *Proc. Natl. Acad. Sci. USA.* **1987**, *84*, 5449.
27. Mor, A.; Nguyen, V. H.; Delfour, A.; Migliore-Samour, D.; Nicolas, P. *Biochemistry* **1991**, *30*, 8824.
28. Lee, S.; Mihara, H.; Aoyagi, H.; Kato, T.; Izumiya, N.; Yamasaki, N. *Biochem. Biophys. Acta.* **1986**, *862*, 211.
29. Mihara, H.; Kammera, T.; Yoshida, M.; Lee, S.; Aoyagi, H.; Kato, T.; Izumiya, N. *Bull. Chem. Soc. Jpn.* **1987**, *60*, 697.
30. Blondelle, S. E.; Houghten, R. A. *Biochemistry* **1992**, *31*, 12688.

Deposition of Ferroelectric $Pb(Zr_{0.52}Ti_{0.48})O_3$ Films on Platinized Silicon Using Nd:YAG Laser

Hoong-Sun Im*, Sang-Hyeob Kim, Young-Ku Choi†, Kee Hag Lee†, and Kwang-Woo Jung*†

Korea Research Institute of Standards and Science, Taeduk Science Town, Taejon 305-600, Korea
†Medicinal Resources Research Center and Department of Chemistry, Wonkwang University, Iksan 570-749, Korea

Lead zirconate titanate (PZT) thin films were deposited onto the $Pt/Ti/SiO_2/Si$ substrate by the pulsed laser deposition with the second harmonic wavelength (532 nm) of Nd:YAG laser. In order to determine the optimum conditions for the film deposition, the phase of the films were investigated as functions of ambient oxygen pressure, substrate temperature, and laser fluence. Also the chemical composition analysis was conducted for the PZT films deposited under various ambient oxygen pressure. When the distance between substrate and bulk PZT target is set to 20 mm, the optimum conditions have been determined to be 3 torr of oxygen pressure, 1.5 J/cm^2 of laser fluence, and 823-848($\pm$10) K range of substrate temperature. At these conditions, perovskite phase PZT films were obtained on platinized silicon. The chemical composition of the films is very similar to that of PZT bulk target. The physical structure of the deposited films analyzed by scanning electron microscopy shows a columnar morphology perpendicular to the substrate surface. Capacitance-Voltage hysteresis loop measurements show also a typical characteristics of ferroelectric thin film. The dielectric constant is found to be 528 for the 0.48 μm thickness of PZT thin film.

Introduction

Recently, thin films of ferroelectric materials with perovskite structure, such as $BaTiO_3$, $PbTiO_3$, and lead-zirconate-titanate (PZT) have attracted considerable attention due to their useful applications in various devices such as piezoelectric vibrator, surface acoustic wave devices, pyroelectric detectors, and nonvolatile random access memories.[1] Such applications require the deposition of these ceramic films onto silicon and the integration of the deposition techniques with semiconductor processing.[2]

A variety of processing modes including rf magnetron sputtering,[3] ion-beam sputtering,[4] electron cyclotron resonance (ECR) plasma stream,[5] sol-gel synthesis,[6] and pulsed laser deposition (PLD)[7] have been used to prepare ferroelectric thin films; among them, PLD has become a very

*Author to whom correspondence should be addressed.

attractive technique for the deposition of multi-element compounds.[8-10] Film deposition by laser ablation is typically accomplished by focusing a high intensity laser beam on a bulk target of the material to be deposited; the interaction of the laser beam with the target produces the flux of evaporated material, *i.e.*, plume, which is deposited onto a heated substrate. The composition of the plume generated by PLD is quite different from that by other evaporation techniques. The main characteristics of PLD are closely related not only to both composition and evolution of the plume but also to the interaction of the ablated species with the ambient gas. The plume by PLD is composed of the species preserving the original stoichiometry of the bulk, which in turn should result in better stoichiometric films.[1] Therefore, the PLD technique has been widely studied as one of the most promising methods for obtaining thin films, specially multicomponent oxides thin films.

Although a systematic investigation of the role of laser fluence, ambient oxygen pressure, and substrate temperature in the ablation process has not been carried out, the comparison of structural properties of the deposited PZT films with the bulk targets indicates that each condition has profound effect on the deposited film quality.[8,11,12] Moreover, it is still unclear whether the ambient oxygen pressure, which is needed to obtain good quality films, is incorporated during the plume evolution or adsorbed directly on the deposited film. In fact, in order to determine the optimum deposition process, detailed studies of the characteristics of the plume are necessary in the ablation regime during the deposition process. However, through the comparison of the properties of deposited films, the choice of the relevant parameters among various deposition conditions is possible.

In this work pulsed laser ablation and deposition method has been used to prepare the perovskite-type PZT thin films onto the platinized silicon substrate. In order to determine the optimum conditions of the deposition process, detailed studies of the influence of the ambient oxygen pressure on the chemical composition and the phase in the deposited films have been performed by analyzing the energy dispersive X-ray measurements and the Glancing X-ray diffraction patterns of deposited PZT films. Also the film structures were compared with those of the bulk target as functions of substrate temperature and laser fluence. In addition, we report the morphological structure and the ferroelectric property of the films deposited at the optimum deposition conditions.

Experimental

A schematic diagram of the experimental apparatus for the preparation of PZT films is shown in Figure 1. The PLD chamber, previously evacuated to 10^{-6} torr, was filled with oxygen to a pressure of 0.1-10 torr before the deposition. Laser radiation was provided by the second harmonic output (532 nm) of a Nd:YAG laser (Quanta-Ray; Model DCR-3) that produces pulses of 10 ns duration at 10 Hz repetition rate. The radiation from the laser was focused to a 1.7×2.4 mm^2 spot on a rotating PZT bulk target. The resulting energy density was 0.7-3 J/cm^2. The laser pulse strikes the target surface at an angle of 45°, and gives rise to the formation of a hot plume[13] consisting of electrons, ions, neutrals, and clusters. During the laser irradiation, the target was rotating at 5-10 rpm in order to avoid crat-erization of the target surface and to eliminate the changes in target composition.

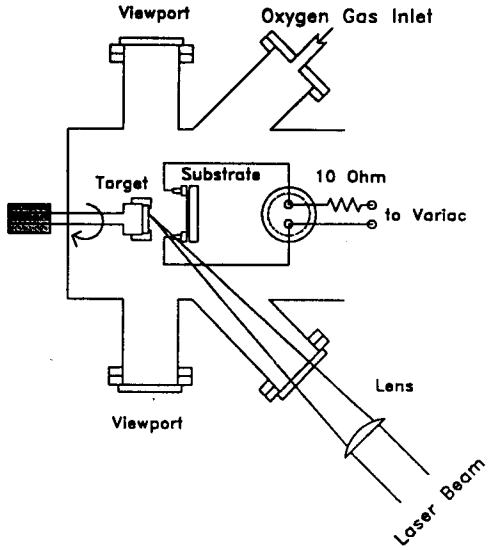

Figure 1. Experimental apparatus for the pulsed laser deposition of PZT thin films.

The bulk targets obtained from the Ssangyong Research Center consists of a single-phase pellet of $Pb(Zr_{0.52}Ti_{0.48})O_3$ with 2 wt.% of SrO. The Pt(300 Å)/Ti(300 Å)/SiO_2(~20 Å)/Si substrate (Chunnam University), mounted parallel to the target at a distance of 20 mm, was held at 773-873($\pm$10) K during film deposition. Pt layer is chosen as a lower electrode and it helps to reduce the lattice mismatch between PZT and Si substrate. In order to enhance the adhesion of Pt to Si oxide, extra Ti layer is also used. These layers could maintain a tolerable barrier effect against PZT.[14] The substrate temperature is estimated by a preliminary measurement using thermocouple and IR-pyrometer. After deposition, the film was annealed for 15 min. The characteristic parameters of the experimental apparatus are listed in Table 1.

The structure and composition of the deposited films were characterized by Glancing X-ray diffraction (GXRD; Rigaku 12KW rotary anode generator) measurements using CuKα radiation and energy dispersive X-ray analyzer (EDXA; Philips LAM1000), respectively. The morphological structure of the deposited films was measured with a scanning electron microscopy (ISID130C). Characterization of electrical property was performed by measuring the capacitance versus bias voltage with a low frequency impedance analyzer (HP4192A).

Results and Discussion

It has been known that the stoichiometric growth of PZT films is difficult due to the high volatility of Pb with respect to the other elements of PZT targets.[12] In order to investigate the effect of ambient oxygen pressure (P_{O2}) on the chemical composition, EDXA analysis was carried out for the PZT films prepared under various ambient oxygen pressures at a laser fluence of 1.5 J/cm^2 and a substrate tem-

Table 1. Characteristic parameters of experimental apparatus for the pulsed laser deposition of PZT thin films

Nd:YAG laser	
Wavelength	532 nm
Pulse duration(fwhm)	10 ns
Repetition rate	10 Hz
Spot dimension	1.7×2.4 mm^2
Energy density	0.7-3 J/cm^2
Target	$Pb(Zr_{0.52}Ti_{0.48})O_3$
Substrate	Pt(300 Å)/Ti(300 Å)/SiO_2(~20 Å)/Si
Target-substrate distance	20 mm
Oxygen pressure	0.01-10 torr
Deposition time	180 sec
Annealing temperature	773-873($\pm$10) K
Annealing time	15 min

perature of 823($\pm$10) K. Figure 2 shows the P_{O2} dependence of the film compositions. The relative abundance of Pb increases significantly with P_{O2}, whereas there is a smooth decrease in the (Zr+Ti) amount. In the low pressure regime, the concentration of Pb is very far from that of the bulk target. These chemical compositions of thin films converge close to those of the bulk target at the P_{O2} of 3 torr. When the P_{O2} is above 3 torr, the Pb amount of the films is larger than that of the bulk target, while the other metal components become lower. These results indicate that the adequate P_{O2} is neccessary in order to match the stoichiometry of the deposited films. The observed improvement of Pb fraction in the films produced at the sufficient ambient oxygen pressure can be ascribed to the fact that re-evaporation of volatile Pb atoms is suppressed by the effective formation of PbO since its vapour pressure is lower than that of Pb. The ablated materials interact with ambient oxygen molecules to produce PbO and also other oxides during the plume propagation from the bulk target to the substrate. Therefore, the formation of PbO and clusters containing Pb in the plume helps to maintain the stoichiometric composition of the film with respect to Pb, the most volatile component.

Figure 3 shows typical GXRD patterns for a bulk ceramic PZT target (top) and for the PZT thin films prepared under various ambient oxygen pressures. PZT thin films were prepared at a laser fluence of 1.5 J/cm^2 and a substrate temperature of 823($\pm$10) K. Based on the JCPDS card number of 33-784, six peaks (2θ=22.05, 31.40, 38.70, 44.85, 50.25, and 55.65) in the spectrum of bulk PZT correspond to the (100), (110), (111), (200), (210), and (211) orientations of perovskite-type structure, which are the typical pattern of tetragonal PZT phase. The thin film prepared at the P_{O2} of 0.01 torr exhibits amorphous structure, indicating that the perovskite type films cannot be obtained from the insufficient P_{O2}. This is confirmed by the result of EDXA analyses. At such a low ambient oxygen pressure the chemical composition of the films should be far from that of the bulk target. As increasing the gas pressure to 0.1 torr, the perovskite phase appears together with unwanted peak (2θ= 29), which is attributed to the lead oxide (PbO) phase. It is evident that this PbO phase is formed due to the deviation of the chemical composition from optimum stoichiometry. At the P_{O2} of 3 torr, the only perovskite phase of PZT film

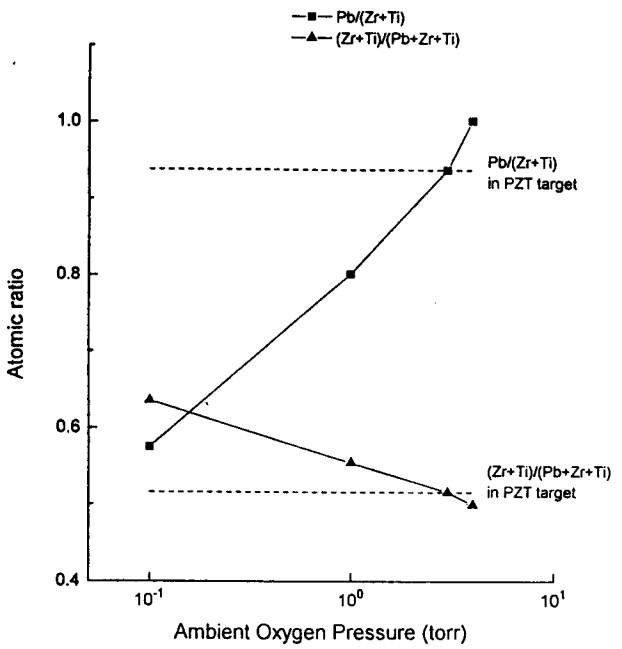

Figure 2. Oxygen background pressure dependence of film compositions, Pb/(Zr+Ti) and (Zr+Ti)/(Pb+Zr+Ti), in PZT films prepared at different oxygen partial pressure: PZT films shown in this figure are prepared at 1.5 J/cm^2 laser fluence, 823 K substrate temperature, and 3 min. deposition time.

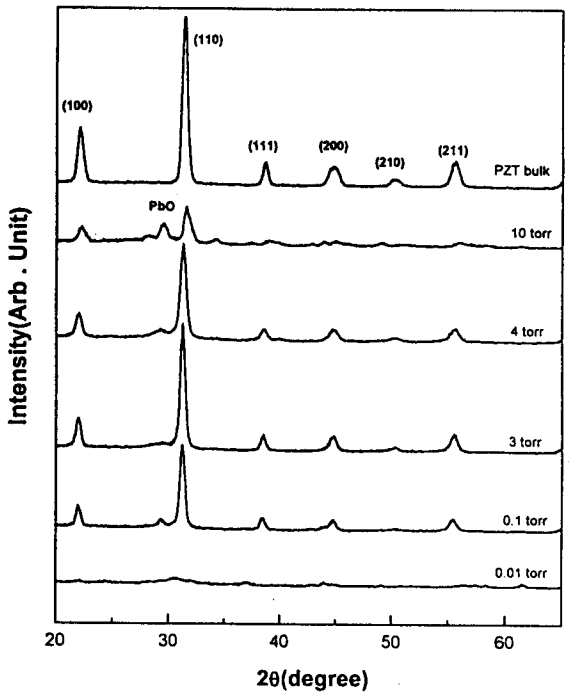

Figure 3. Glancing X-ray diffraction patterns of the PZT thin films deposited at the same conditions in Figure 2.

is obtained (see figure 3). When the pressure increases more than 3 torr, however, the peak for PbO phase appears again in the GXRD pattern. At 10 torr, the film exhibits poor crystalline structure containing PbO phase. Furthermore, the formation of PbO phase competes with the growth of (110) orientation of PZT film since the increase

of PbO phase causes the reduction of (110) peak intensity (see figure 3).

The results from EDXA and GXRD indicate that the P_{O2} controls the amounts of metal elements and also the phase of the film. The results suggest that with the given laser fluence and substrate temperature there is an optimum pressure of P_{O2} for obtaining the perovskite phase of PZT film. In the present experiment, it is known that the formation of PbO phase originates probably from the deficiency and excess of the P_{O2} during the deposition. That is, the deviation of the stoichiometric composition causes the formation of PbO phase in the deposited films.

In a recent study on the diagnostics of the ejected species in the laser ablation of PZT targets by time-of-flight mass spectrometry (TOFMS), fluorescence spectroscopy, and covariance mapping technique, Amoruso *et al.*[15] reported that the ionized part of the plume is restricted to the range 5-10%. They also concluded that the ions possess higher kinetic energy than the neutrals and such high energy ions stimulate the epitaxial growth by creating crystalline centers. The role of the ions on the achievement of a good quality deposition is not yet completely clear; however, the high reactivity of the charged species is expected to enhance the collisional processes during the plasma expansion. This collisional processes are responsible for the formation of molecular oxides and small clusters which are considered relevant for the attainment of the required chemical composition and the phase in the deposited films.[15-18]

Our results obtained from the studies by EDXA and GXRD also confirm that the ambient oxygen pressure plays an important role both in the capture of oxygen required to obtain the correct stoichiometric composition of the deposited film and in the formation of the perovskite phase by producing various oxides (such as PbO, PbTiO, TiO, etc) and their clusters originating from the interaction between the ablated species and oxygen molecules.

The substrate temperature influences drastically the crystal structure of deposited films. Figure 4 shows GXRD patterns of the deposited films at different substrate temperatures in the range 773-873($\pm$10) K. The laser fluence and P_{O2} were 1.5 J/cm^2 and 3 torr, respectively. The film grown at temperature lower than 773($\pm$10) K consisted of only a PbO phase. At about 823($\pm$10) K the film contains the perovskite single phase of PZT. The patterns are not so different for the thin films grown between 823($\pm$10) K and 848($\pm$10) K, which show a perfect perovskite structure of PZT. Above 848($\pm$10) K the PbO phase appears again with the PZT perovskite phase. The appearance of PbO phase at below 823 K and above 848 K causes from the combination of the retained Pb and O in the present PZT pervoskite structure because of the stoichiometric deviation. The result indicates that the processing window for *in-situ* deposition of perovskite phase of PZT is narrow with substrate temperature of 823-848($\pm$10) K.

GXRD measurement is carried out for PZT films prepared under various laser fluences at a substrate temperature of 823($\pm$10) K and the P_{O2} of 3 torr (see Figure 5). The film deposited below 1 J/cm^2 of the laser fluence has a large amount of the PbO structure compared with the perovskite one, though above this fluence, the perovskite structure becomes dominant in the deposited films. Further

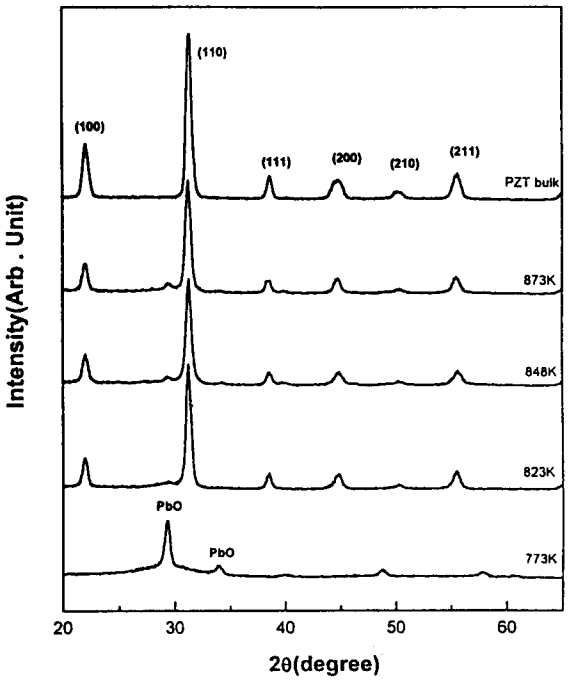

Figure 4. GXRD patterns of deposited films as a function of substrate temperature. The error term of the temperature is omitted intentionally in the figure for convenience. The PZT films are prepared at 1.5 J/cm^2 laser fluence, 3 torr oxygen pressure, and 3 min. deposition time.

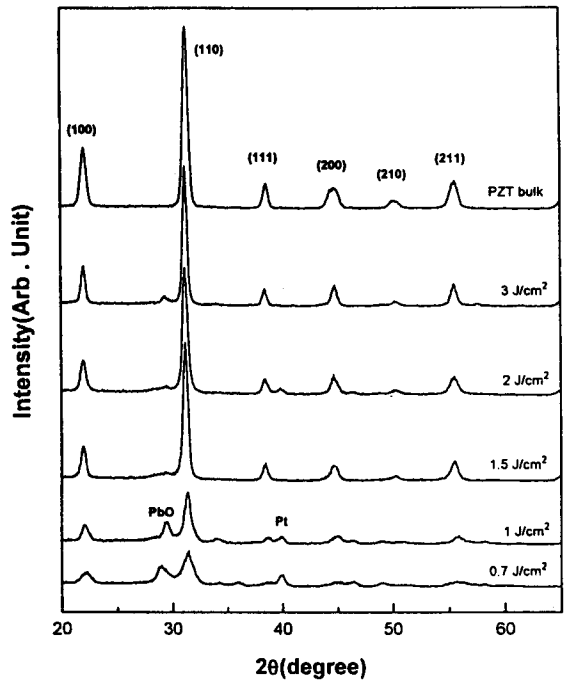

Figure 5. GXRD patterns of deposited films at different laser fluences. The PZT films are prepared at 823($\pm$10) K substrate temperature, 3 torr oxygen pressure, and 3 min. deposition time.

increase of laser fluence causes the PbO phase in the deposited films due to the compositional variations.[19] The laser fluence has a profound effect on the deposited film quality because small fluctuations of the laser fluence result in

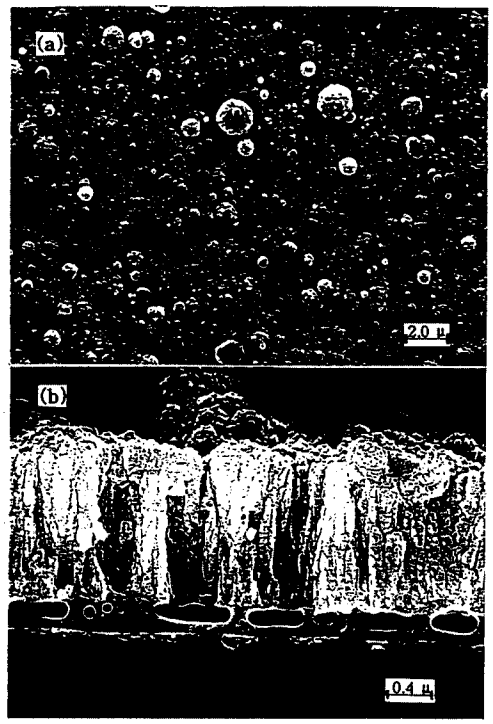

Figure 6. SEM photographs of a surface (top) and cross section (bottom) of PZT films deposited at the optimum conditions, *i.e.*, 1.5 J/cm^2 laser fluence, 3 torr oxygen pressure, 823(±10) K substrate temperature, and 3 min. deposition time. The scale of the top and bottom photographs are 2 μm and 0.4 μm, respectively.

the compositional changes within the plume and consequently in its interaction with the oxygen molecules.[20] Though a systematic investigation of the influence of laser energy on the deposition process has not been carried out, several authors,[19,21-23] have shown that the superconducting films of the good quality are obtained when the energy density of the laser is equal or larger than 2 J/cm^2, which is in reasonable agreement with our present result of 1.5 J/cm^2 for PZT thin films.

The morphology of the deposited films was analyzed by scanning electron microscopy (SEM) of surfaces and cross sections of the films. SEM photographs of deposited film prepared at the laser fluence of 1.5 J/cm^2, the substrate temperature of 823(±10) K, and the P_{O2} of 3 torr are shown in Figure 6. Although the droplets, or particulates, of less than a couple of micrometer are randomly distributed over the film surface, deposited PZT films are found to have a smooth surface and a dense structure. Droplet formation is the most important issue to be solved for the application of films prepared by laser ablation. Droplet formation is ascribed to the fact that the ejected clusters are not decomposed efficiently during the propagation of the plume towards the substrate.[24] The films were also found to be permeated with microcracks in some areas. A relative difference in thermal expansion coefficients between PZT film (2.5×10^{-6} °C^{-1}) and Pt layer (8.9×10^{-6} °C^{-1}) of platinized substrate can result in cracks during the annealing process.[25] However, evaporation of excess lead oxide from the grain boundaries has also been shown to cause cracking during grain densification.[26] The cross sectional view of the

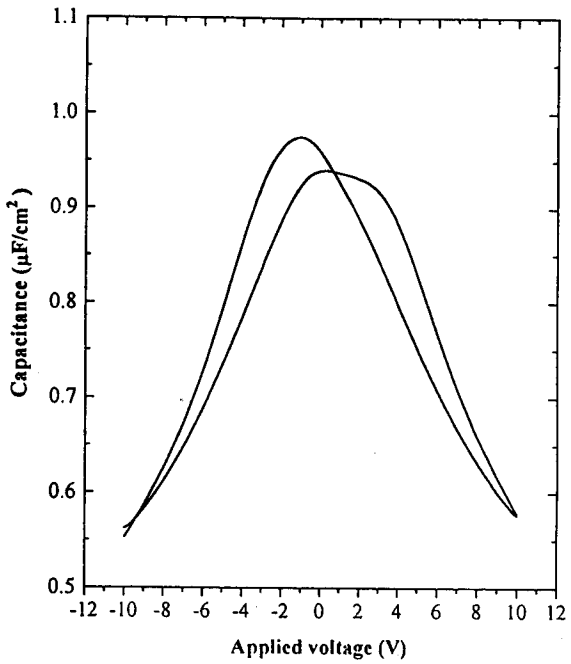

Figure 7. Capacitance *vs* voltage curves for the PZT film deposited at optimum condition. The test was performed with an impedance analyzer using an ac excitation voltage of 100 KHz and a scan interval of 0.2 V/step at room temperature.

film shows a columnar morphology perpendicular to the surface. The columnar structures are seen to grow on top of a Pt layer and are fairly regularly spaced. From the film thickness the deposition rate is calculated to be in the range of 80 per second, which is at least two orders of magnitude greater than that of magnetron sputtering.[27]

Electrical measurement of capacitance versus bias voltage across the film was performed to characterize the electrical behavior of the deposited PZT film. Figure 7 displays the capacitance C versus bias voltage V measured at room temperature with an impedance analyzer. The deposited films show high resistance and low dissipation factors, which are the typical features of high dielectric thin films. The capacitance showed two peaks on either side of the abscissa (dc bias). The capacitance peaks and the corresponding hysteresis loops are characteristic of well-behaved PZT films as revealed by the good symmetry in the hysterectic curve shown in the figure. This measurement indicates that the conduction of PZT films deposited by laser ablation is similar to that observed in films produced by other techniques. The dielectric constant of the deposited films having a thickness of 0.48 μm was determined to be 528.

Conclusion

PZT thin films of perovskite phase were successfully prepared by pulsed laser ablation of a stoichiometric bulk target. The structure, chemical composition, and electrical property of the deposited films are clearly dependent on the oxygen background pressure, laser fluence, and substrate temperature. The films deposited at the optimum conditions exhibited good ferroelectric properties. Work is in progress to elucidate the mechanisms controlling the synthesis of PZT

films and to understand the ablation process and chemical reactivity of ejected species during the plume expansion and propagation.

Acknowledgment. H.-S. Im acknowledges the financial support from Ministry of Science and Technology. This work is supported by the non-directed research fund, the Korea Research Foundation, 1996, which is gratefully acknowledged. We deeply appreciate the efforts of Dr. H. K. Kim in KRISS and Prof. Woo in Chunnam Univ. for preparing the platinized subsrates and the helpful discussion of Mr. Y. I. Kim on this work.

References

1. Dijkamp, D.; Venkatesan, T.; Wu, X. D.; Sahen, S. A.; Jisrawi, S.; Min-Lee, Y. H.; McLean, W. L.; Croft, M. *Appl. Phys. Lett.* **1987**, *51*, 660.
2. Scott, J. F.; Pa de Araujo, C. A. *Science* **1989**, *246*, 1400.
3. Krupanidhi, S. B.; Maffei, N.; Sayer, M.; El-Assal, K. *J. Appl. Phys.* **1983**, *54*, 6601.
4. Castellano, R. N.; Feinstein, L. G. *J. Appl. Phys.* **1979**, *50*, 4406.
5. Okuyama, M.; Togani, Y.; Hamakawa, Y. *Appl. Surf. Sci.* **1988**, *33/34*, 625.
6. Payne, D. A. *Bull. Am. Phys. Soc.* **1989**, *34*, 991.
7. Otsubo, S.; Maeda, T.; Minamikawa, T.; Yonezawa, Y.; Morimoto, A.; Shimizu, T. *Jpn. J. Appl. Phys.* **1989**, *29*, L133.
8. Roy, D.; Kupranidhi, S. B.; Dougherty, J. P. *J. Appl. Phys.* **1991**, *69*, 7930.
9. Kidoh, H.; Ogawa, T.; Morimoto, A.; Shimizu, T. *Appl. Phys. Lett.* **1991**, *58*, 2910.
0. Ramesh, R.; Luther, K.; Wilkens, B.; Hart, D. L.; Wang, E.; Tarascon, J.; Inam, A.; Wu, X. D.; Venkatesan, T. *Appl. Phys. Lett.* **1990**, *57*, 1505.
11. Lee, J.; Safari, A.; Pfeffer, R. L. *Appl. Phys. Lett.* **1992**, *61*, 1643.
12. Horwitz, J. S.; Grabowski, K. S.; Chrisey, D. B.; Leuchtner, R. E. *Appl. Phys. Lett.* **1991**, *59*, 1565.
13. Ready, J. F. *J. Appl. Phys. 1965*, *36*, 462.
14. Abe, K.; Tomita, H.; Toyoda, H.; Imai, M.; Yokote, Y. *Jpn. J. Appl. Phys.* **1991**, *30*, 2152.
15. Amoruso, S.; Berardi, V.; Dente, A.; Spinelli, N.; Armenante, M.; Volott, R.; Fuso, F.; Allegrini, M.; Arimondo, E. *J. Appl. Phys.* **1995**, *78*, 494.
16. Masciarelli, G.; Fuso, F.; Allegrini, M.; Arimondo, E. *J. Mol. Spectrosco.* **1992**, *153*, 96.
17. Gupta, A. *J. Appl. Phys.* **1993**, *73*, 7877.
18. Iembo, A.; Fuso, F.; Allegrini, M.; Arimondo, E.; Berardi, V.; Spinelli, N.; Leccabue, F.; Watts, B. E.; Franco, G.; Chiorboli, G. *Appl. Phys. Lett.* **1993**, *63*, 1194.
19. Singh, R. K.; Holland, O. W.; Narayan, J. *J. Appl. Phys.* **1990**, *68*, 223.
20. Berardi, V.; Amoruso, S.; Spinelli, N.; Armenante, M.; Velotta, R.; Fuso, F.; Allegrini, M.; Arimondo, E. *J. Appl. Phys.* **1994**, *76*, 8077.
21. Singh, R. K.; Narayan, J. *Phys. Rev.* **1990**, *A41*, 8843.
22. Kim, H. S.; Kwok, H. S. *Appl. Phys. Lett.* **1992**, *61*, 2234.
23. Wu, X. D.; Inam, A.; Venkatesan, T.; Chang, C. C.; Chase, E. W.; Barboux, P.; Tarascon, J. M.; Wilkens, B. *Appl. Phys. Lett.* **1988**, *52*, 752.
24. Koren, G.; Gupta, A.; Baseman, R.J.; Lutwyche, M. I.; Laibowitz, R. B. *Appl. Phys. Lett.* **1989**, *55*, 2450.
25. Sreenivas, K.; Sayer, M.; Garrett, P. *Thin Solid Films* **1989**, *172*, 251.
26. Sayer, M. in *Proceedings of the 6th IEEE International Symposium of Applications of Ferroelectrics*; June 8-11, 1986, Bethlehem, PA, edited by Wood, V. E.; IEEE, New York, 1986; pp 560-568.
27. Sreenival, K.; Sayer, M. *J. Appl. Phys.* **1988**, *64*, 1484.

Electrochemical Properties of $Li_xCo_yNi_{1-y}O_2$ Prepared by Citrate Sol-Gel Method

Soon Ho Chang, Seong-Gu Kang, and Kee Ho Jang

Electronics and Telecommunications Research Institute, Taejon 305-600, Korea
Received September 6, 1996

The electrochemical properties of $Li_xCo_yNi_{1-y}O_2$ compounds (y=0.1, 0.3, 0.5, 0.7, 1.0) prepared by citrate sol-gel method have been investigated. The $Li_xCo_yNi_{1-y}O_2$ compounds were annealed at 850 °C for 20 h after preheating at 650 °C for 6 h, in air. The x-ray diffraction (XRD) patterns for $Li_xCo_yNi_{1-y}O_2$ have shown that these compounds have a well developed layered structure ($R\bar{3}\,m$). From the scanning electron microscopy of $Li_xCo_yNi_{1-y}O_2$, particle size was estimated less than 5 μm. The $Li//Li_xCo_yNi_{1-y}O_2$ electrochemical cell consists of Li metal anode and 1 M $LiClO_4$-propylene carbonate (PC) solution as the electrolyte. The differences in intercalation rate of the $Li_xCo_yNi_{1-y}O_2$ in the first charge/discharge cycle were less than 0.05 e^-. The first discharge capacities of Li_xCoO_2 and $Li_xCo_{0.3}Ni_{0.7}O_2$ were ~130 mAh/g and ~160 mAh/g, respectively.

Introduction

$LiNiO_2$,[1-6] $LiCoO_2$,[7-15] $LiMn_2O_4$,[16-19] and $Li_xCo_yNi_{1-y}O_2$[20-24] have been intensively studied as cathode active materials in lithium secondary batteries. Among them, $LiNiO_2$, $LiCoO_2$, and $Li_xCo_yNi_{1-y}O_2$ are isostructural with α-$NaFeO_2$. In these